

Short Communication

Study on the Improvement of Rate Capability of Spinel $\text{Li}_4\text{Ti}_5\text{O}_{12}$ with Graphene/Carbon Nanotubes Binary Conductive Additive

Xing Li^{1,2,*}, Pengxiao Huang¹, Hui Peng¹, Ying Zhou^{1,2}, Wen Li³, Meizhen Qu^{3,*}

¹ School of Materials Science and Engineering, Southwest Petroleum University, Chengdu 610500, China

² State Key Laboratory of Oil and Gas Reservoir Geology and Exploitation, Southwest Petroleum University, Chengdu 610500, China

³ Chengdu Institute of Organic Chemistry, Chinese Academy of Science, Chengdu 610041, China

*E-mail: lixing@swpu.edu.cn; mzhqu@cioc.ac.cn

Received: 22 June 2014 / Accepted: 17 July 2014 / Published: 25 August 2014

A graphene/CNTs binary conductive additive was synthesized by in situ reducing the graphite oxide/CNTs mixture in Ar atmosphere. The binary conductive additive consists of graphene nanosheets and CNTs, which could more efficiently improve the electronic conductivity of the spinel $\text{Li}_4\text{Ti}_5\text{O}_{12}$ than that using single graphene or CNTs as conductive additive. The $\text{Li}_4\text{Ti}_5\text{O}_{12}$ using the graphene/CNTs as conductive additive exhibits excellent rate capability. At 0.2 C, its initial discharge specific capacity is 172 mAh/g, which is close to the theoretical value of the spinel $\text{Li}_4\text{Ti}_5\text{O}_{12}$ (175 mAh/g). And even at the high rate of 5.0 C, 10.0 C and 20.0 C, it can still remain at 147 mAh/g, 136 mAh/g and 110 mAh/g, respectively.

Keywords: graphene/CNTs; binary conductive additive; spinel lithium titanate; rate capability; lithium ion batteries

1. INTRODUCTION

Lithium ion batteries (LIBs) have gained commercial success and conquered the portable market for some of their outstanding properties, such as high energy density and friendliness to the environment. Recently, LIBs are also expected to be a promising power source for automobiles, such as electric vehicles (EV), hybrid vehicles (HEV) and plug-in hybrid vehicles (PHEV) [1, 2]. In order to meet the demand for the application of LIBs as the power source for automobiles, the electrode active materials of LIBs should have high capacity, excellent cycling performance and good rate capability [3, 4].

Spinel lithium titanate ($\text{Li}_4\text{Ti}_5\text{O}_{12}$) has been demonstrated as a potential candidate for the anode electrode material in lithium ion batteries because it has some unique characteristics such as good thermal stability, high safety and unlimited cycle life [5-8]. However, as $\text{Li}_4\text{Ti}_5\text{O}_{12}$ is an insulator, the low electrical conductivity (ca. $10^{-13} \text{ S cm}^{-1}$) makes it suffer from the problem of poor rate capability [9], which is unfavorable to power density of the LIBs that using $\text{Li}_4\text{Ti}_5\text{O}_{12}$ as anode material. In order to overcome the low electrical conductivity and further improve the rate capability of $\text{Li}_4\text{Ti}_5\text{O}_{12}$, several methods have been developed. These include synthesizing nanosized $\text{Li}_4\text{Ti}_5\text{O}_{12}$ particles [10], doping $\text{Li}_4\text{Ti}_5\text{O}_{12}$ with aliovalent metal ions [11] and forming a composite of $\text{Li}_4\text{Ti}_5\text{O}_{12}$ and a conductive second phase such as metal, C and polyacene [12-14].

In addition to the above mentioned methods, using different conductive additives to improve the electronic conductivity of the $\text{Li}_4\text{Ti}_5\text{O}_{12}$ is also an effective approach [15]. Carbon black and graphite powders have been widely used as conductive additives owing to their high electrical conductivity and chemical inertness [16]. Moreover, graphene and carbon nano-tubes (CNTs) are also recognized as ideal conductive additives for their extraordinary electronic transport property, flexible structure, high mechanical strength and high surface area. Recently, researchers reported that binary conductive additives such as mesoporous carbon/carbon black and CNTs/carbon black have shown some superiority over single conductive additives [17, 18]. However, few works focused on the conductive additives of the graphene and the CNTs, especially for the graphene/CNTs binary conductive additive. In the present work, we synthesized a graphene/CNTs binary conductive additive by in situ reducing the graphite oxide/CNTs mixture under Ar atmosphere, and studied on the improvement of rate capability of spinel $\text{Li}_4\text{Ti}_5\text{O}_{12}$ with the binary conductive additive. For comparison, the graphene and CNTs as single conductive additive to improve the rate capability of the $\text{Li}_4\text{Ti}_5\text{O}_{12}$ were also studied, respectively. The novelty of this paper is listed as following: (1) we synthesized a graphene/CNTs composite via in situ reducing the graphite oxide/CNTs mixture under Ar atmosphere; (2) the graphene/CNTs composite was used as binary conductive additive to improve the rate capability of the $\text{Li}_4\text{Ti}_5\text{O}_{12}$, and the binary conductive additive could more efficiently improve the rate capability of $\text{Li}_4\text{Ti}_5\text{O}_{12}$ than that of the single graphene or CNTs conductive additive.

2. EXPERIMENTAL

2.1. Material synthesis

The graphene/CNTs binary conductive additive was obtained via reducing the graphite oxide/CNTs mixture at 1100°C in Ar atmosphere. The graphite oxide was prepared by the oxidation of natural crystalline flake graphite using the Hummers method [19]. Then, the above obtained graphite oxide slurry was mixed with CNTs using Polyvinylpyrrolidone (PVP) as dispersant to form a uniform mixture. Finally, the mixture was dried at 80°C and reduced at 1100°C in Ar atmosphere to obtain the graphene/CNTs binary conductive additive. The mass ratio of the graphene and CNTs in the binary conductive additive was given as 3:1. The graphene used in the present work was also prepared via reducing the graphite oxide mentioned above at 1100°C in Ar atmosphere. The CNTs are multiwall,

with a diameter and length of about 20–30 nm and 2–3 μm respectively, which were purchased from Chengdu Organic Chemicals Co., Ltd. The $\text{Li}_4\text{Ti}_5\text{O}_{12}$ used in the present study is commercial, which was donated by Chengdu Xingneng New Materials Co., LTD.

2.2. Materials characterization

The microstructural morphologies of the graphene/CNTs binary conductive additive, the graphene and the CNTs were observed by scanning electronic microscopy (SEM FEI INSPECT-F).

2.3. Electrochemical measurements

The rate capability of the $\text{Li}_4\text{Ti}_5\text{O}_{12}$ that using graphene/CNTs, graphene and CNTs as conductive additives were measured by means of two-electrode coin-type half cells (CR2032). The working electrodes consist of 90 wt.% $\text{Li}_4\text{Ti}_5\text{O}_{12}$ active material, 5 wt.% conductive additive and 5 wt.% LA-132 binder, the counter electrode was lithium foil. The separator was Celgard 2400, and the electrolyte was 1 M $\text{LiPF}_6/\text{EC}:\text{DEC}:\text{DMC}$ (1:1:1 in volume). The cells were assembled in a glove box filled with high purity argon gas. Galvanostatic discharge–charge measurements were carried out under different current densities at constant cut-off voltages of 1–3 V at room temperature (NEWARE Electronic Co. Ltd, China). The AC impedance spectrum was measured by using a Solatron 1260 Impedance Analyzer in the frequency range 10^{-2} – 10^6 Hz with a potential perturbation at 10 mV.

3. RESULTS AND DISCUSSION

Fig.1 (a) shows the SEM image of the graphene/CNTs binary conductive additive, and the close-up SEM image of the binary conductive additive is shown in Fig.1(b). From Fig.1(a), it can be observed that the graphene and the CNTs were evenly mixed, moreover, the CNTs acting like bridges, which connect the graphene nanosheets and give a effective conductive net. Furthermore, Fig.1(b) also shows that the CNTs could insert into the layers of the graphene nanosheets, and the graphene and the CNTs all exhibit less agglomeration. The above results indicate that the graphene/CNTs binary conductive additive could be easily dispersed into the electrode [20], and it could more effectively improve the electronic conductivity of the $\text{Li}_4\text{Ti}_5\text{O}_{12}$. Fig.1 (c) shows the SEM image of the graphene prepared in this study, from which it could be observed that the as prepared graphene looks transparent, which suggests that it has excellent electronic conductivity [21, 22]. Moreover, the diameter of the graphene is more than 5 μm , and the microstructure characteristics of the graphene nanosheets are thin and few layers. Fig.1 (d) is the SEM image of the CNTs used in this study. There, it can be observed that the diameter and length of the CNTs are about 20–30 nm and 2–3 μm , respectively.

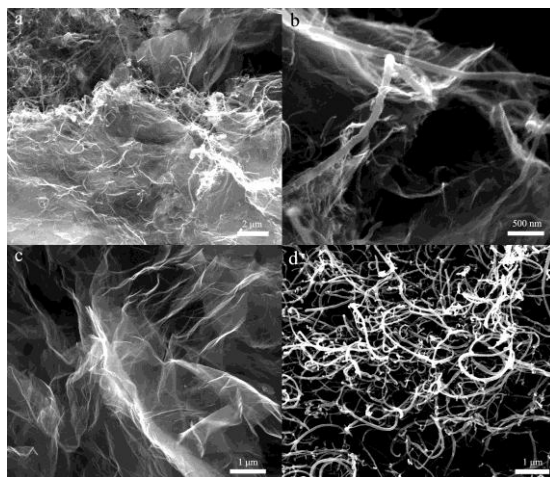


Figure 1. SEM images of the graphene/CNTs binary conductive additive (a), (b), graphene (c) and CNTs (d).

Fig.2 shows the AC impedance spectra of the $\text{Li}_4\text{Ti}_5\text{O}_{12}$ electrodes with graphene/CNTs, graphene and CNTs as conductive additive. The $\text{Li}_4\text{Ti}_5\text{O}_{12}$ electrodes with different conductive additives were measured at the stable voltage of 1.55 V. The AC impedance spectra of the electrodes were simulated by Z-view software using the same equivalent circuit. It can be observed from Fig.2 that the experimental and simulated AC impedance spectra are almost coincident, which indicates that the AC impedance spectra of the electrodes all fit the equivalent circuit. According to the equivalent circuit, the depressed semicircle at high-middle frequency range represent the particle/electrolyte interface charge transfer resistance (R_{ct}), the slope line at low frequency corresponds to the Warburg impedance (Z_w), the R_s is the resistance of the electrolyte, the constant phase element (CPE) is placed to represent the double-layer capacitance and the C_L is the insertion capacitance at the applied potential [23, 24]. The parameters of the recorded equivalent circuit are shown in Table 1, from which it can be observed that the R_{ct} of the $\text{Li}_4\text{Ti}_5\text{O}_{12}$ electrode with graphene as conductive additive is smaller than that of the electrode with CNTs as conductive additive, and the $\text{Li}_4\text{Ti}_5\text{O}_{12}$ electrode with graphene/CNTs as conductive additive has the smallest R_{ct} among the electrodes. Moreover, the parameters of the exchange current densities ($i^0 = RT/nFR_{ct}$) [25] also show that the $\text{Li}_4\text{Ti}_5\text{O}_{12}$ electrode with graphene/CNTs as conductive additive has the biggest i^0 value. These results indicate that the graphene/CNTs binary conductive additive could more efficiently improve the charge/transfer kinetics of the $\text{Li}_4\text{Ti}_5\text{O}_{12}$ than that of the single graphene or CNTs conductive additive, which should be ascribed to that the $\text{Li}_4\text{Ti}_5\text{O}_{12}$ electrode that using graphene/CNTs as conductive additive could form more effectively conductive nets for CNTs in the electrode acting like bridges which could connect the isolated $\text{Li}_4\text{Ti}_5\text{O}_{12}$ particles and the graphene nanosheets. Furthermore, the fact of the $\text{Li}_4\text{Ti}_5\text{O}_{12}$ electrode that using graphene as conductive additive has better charge/transfer kinetics than that of using CNTs as conductive additive should be attributed to that the graphene conductive additive has bigger BET surface area than that of the CNTs, which could give more effective contact with the $\text{Li}_4\text{Ti}_5\text{O}_{12}$ particles.

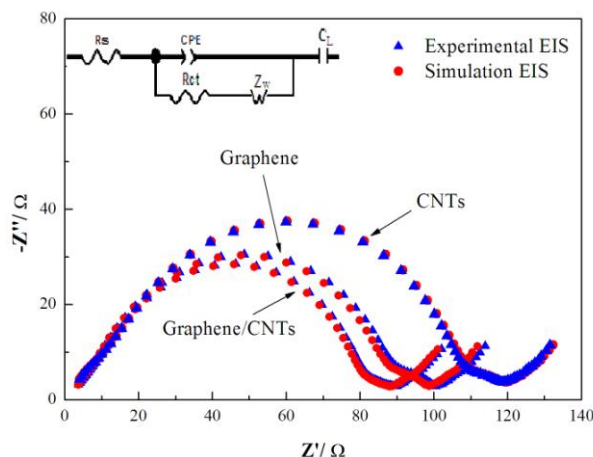


Figure 2. AC impedance spectra with the equivalent circuit of the Li₄Ti₅O₁₂ electrodes using graphene/CNTs, graphene and CNTs as conductive additive.

Table 1. Impedance parameters calculated from equivalent circuits.

Conductive Additive	R _s (Ω)	R _{ct} (Ω)	i ^o (mA/cm ²)
Graphene/CNTs	2.221	85.2	0.303
graphene	2.348	98.5	0.262
CNTs	2.535	116.4	0.221

Fig.3 shows the cyclic performances of the Li₄Ti₅O₁₂ electrodes using graphene/CNTs, graphene and CNTs as conductive additive at different rates from 0.2 C, 0.5 C, 1.0 C, 3.0 C, 5.0 C, 10.0 C and 20.0 C between 1 V and 3 V. The charge-discharge processes of the samples are carried out for 3 cycles at 0.2 C and for 10 cycles at other different rates mentioned above, respectively. From Fig.3, it can be observed that the Li₄Ti₅O₁₂ electrode using graphene/CNTs as conductive additive exhibits the highest discharge specific capacity especial at high rates as compared with the Li₄Ti₅O₁₂ electrode using graphene or CNTs as conductive additives. At 0.2 C, its initial discharge specific capacity is 172 mAh/g, which is close to the theoretical value of the spinel Li₄Ti₅O₁₂ (175 mAh/g). At 5.0 C and 10.0 C, it is 147 mAh/g and 136 mAh/g; and even at 20.0 C, it can still remain at 110 mAh/g. Furthermore, as shown in Fig.3, it could be observed that the Li₄Ti₅O₁₂ electrode using graphene as conductive additive exhibits higher discharge specific capacity at different rates than that of the Li₄Ti₅O₁₂ electrode using CNTs as conductive additives. At 0.2 C, its initial discharge specific capacity is 168 mAh/g; at 5.0 C and 10.0 C, it is 139 mAh/g and 118 mAh/g; and even at 20.0 C, it can still remain at 88 mAh/g. However, for the Li₄Ti₅O₁₂ electrode using CNTs as conductive additives, at 0.2 C, its initial discharge specific capacity is 163 mAh/g; at 5.0 C and 10.0 C, it quickly decay to 67 mAh/g and 44 mAh/g; and while at 20.0 C, it can only remain at 22 mAh/g. These results indicate that the graphene/CNTs binary conductive additive could more efficiently improve the rate capability of the Li₄Ti₅O₁₂ than that of single graphene or CNTs conductive additive, which should be ascribed to

that the graphene/CNTs binary conductive additive could form more effectively conductive nets and make the electrode have highest charge/transfer kinetics.

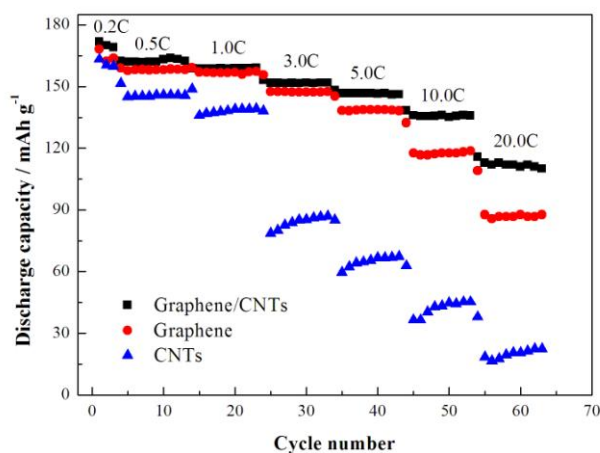


Figure 3. Discharge specific capacity of the $\text{Li}_4\text{Ti}_5\text{O}_{12}$ electrodes using graphene/CNTs, graphene and CNTs as conductive additive at different rates.

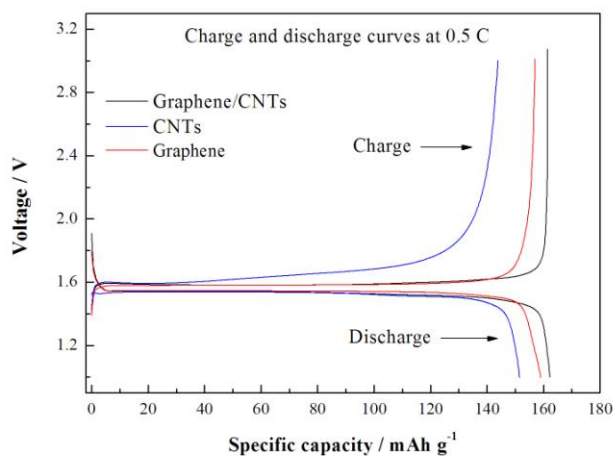


Figure 4. Discharge and charge curves of the $\text{Li}_4\text{Ti}_5\text{O}_{12}$ electrodes using graphene/CNTs, graphene and CNTs as conductive additive at 0.5 C.

Furthermore, as shown in Fig.4 and Fig.5, the margins between the charge and discharge plateau potentials of the $\text{Li}_4\text{Ti}_5\text{O}_{12}$ electrode that using graphene/CNTs as conductive additive are obviously smaller than those using single graphene or CNTs as conductive additives at 0.5 C and 5.0 C, which suggests that the $\text{Li}_4\text{Ti}_5\text{O}_{12}$ electrode using graphene/CNTs as conductive additive has the smallest electrode polarization. These results also indicate that the graphene/CNTs binary conductive additive could more efficiently improve the electronic conductivity of the spinel $\text{Li}_4\text{Ti}_5\text{O}_{12}$ than those using single graphene or CNTs as conductive additive.

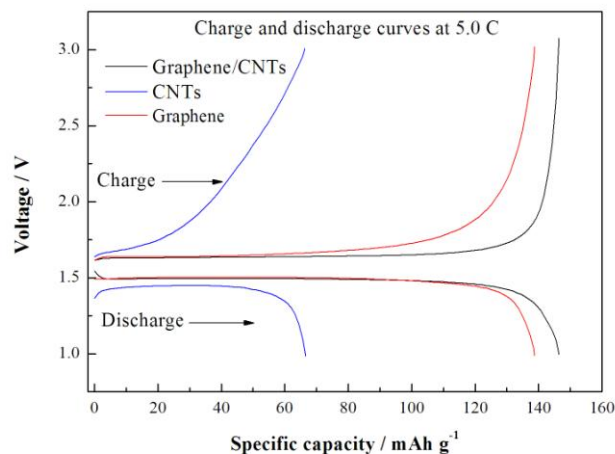


Figure 5. Discharge and charge curves of the $\text{Li}_4\text{Ti}_5\text{O}_{12}$ electrodes using graphene/CNTs, graphene and CNTs as conductive additive at 5.0 C.

4. CONCLUSIONS

We synthesized a graphene/CNTs binary conductive additive by in situ reducing the graphite oxide/CNTs mixture under Ar atmosphere, and studied on the improvement of rate capability of spinel $\text{Li}_4\text{Ti}_5\text{O}_{12}$ with the binary conductive additive. For comparison, the graphene and CNTs as single conductive additive to improve the rate capability of the $\text{Li}_4\text{Ti}_5\text{O}_{12}$ were also studied, respectively. The results indicate that the graphene/CNTs binary conductive additive could more efficiently improve the electronic conductivity of the spinel $\text{Li}_4\text{Ti}_5\text{O}_{12}$ than those using single graphene or CNTs as conductive additive. The $\text{Li}_4\text{Ti}_5\text{O}_{12}$ electrode using graphene/CNTs as conductive additive exhibits the best rate capability. We believed that should be ascribed to that the graphene/CNTs binary conductive additive could give more effectively conductive nets in the $\text{Li}_4\text{Ti}_5\text{O}_{12}$ electrode than that of single graphene or CNTs conductive additive.

ACKNOWLEDGEMENTS

This work was carried out with financial support from the National Natural Science Foundation of China (No. 51302232), the Ministry of Science and Technology of the People's Republic of China (No. 2011CB932604), the Education Department of Sichuan Province (No. 13ZB0205), and the Innovative Research Team of Southwest Petroleum University (No. 2012XJZT002).

References

1. B. Scrosati, *Nature* 373 (1995) 557–558.
2. A. S. Arico, P. Bruce, B. Scrosati, J. M. Tarascon, W. V. Schalkwijk, *Nat. Mater.* 4 (2005) 366–377.
3. M. Armand, J.M. Tarascon, *Nature* 451 (2008) 652–657.
4. B. Kang, G. Ceder, *Nature* 458 (2009) 190–193.

5. K. Wu, J. Yang, X.Y. Qiu, J.M. Xu, Q.Q. Zhang, J. Jin, Q.C. Zhuang, *Electrochim. Acta* 108 (2013) 841–851.
6. M. Marinaro, F. Nobili, A. Birrozzì, S.K. Eswara Moorthy, U. Kaiser, R. Tossici, R. Marassi, *Electrochim. Acta* 109 (2013) 207–213.
7. J.Y. Liao, X.C. Xiao, D. Higgins, D.G. Lee, *Electrochim. Acta* 108 (2013) 104–111.
8. Y. Ding, G.R. Li, C.W. Xiao, X.P. Gao, *Electrochim. Acta* 102 (2013) 282–289.
9. X. Li, M.Z. Qu, Y.J. Huai, Z.L. Yu, *Electrochim. Acta* 55 (2010) 2978–2982.
10. X.R. Li, H. Hu, S. Huang, G.G. Yu, L. Gao, H.W. Liu, Y. Yu, *Electrochim. Acta* 112 (2013) 356–363.
11. W. Xu, X.L. Chen, W. Wang, D. Choi, F. Ding, J.M. Zheng, Z.M. Nie, Y. J. Choi, J.G. Zhang, Z.G. Yang, J.C. Jumas, *J. Power Sources* 236 (2013) 169–174.
12. W. Wang, Y.Y. Guo, L.X. Liu, S.X. Wang, X.J. Yang, H. Guo, *J. Power Sources* 245 (2014) 624–629.
13. W. Fang, X.Q. Cheng, P.J. Zuo, Y.L. Ma, G.P. Yin, *Electrochim. Acta* 93 (2013) 173–178.
14. H.Y. Yu, X.F. Zhang, A.F. Jalbout, X.D. Yan, X.M. Pan, H.M. Xie, R.S. Wang, *Electrochim. Acta* 53 (2008) 4200.
15. R. Dominko, M. Gaberšček, J. Drogenik, M. Bele, J. Jamnik, *Electrochim. Acta* 48 (2003) 3709.
16. Jin K. Hong, Jong H. Lee, Seung M. Oh, *Journal of Power Sources* 111 (2002) 90.
17. Qingtang Zhang, Gongchang Peng, Guoping Wang, Meizhen Qu, Zuo Long Yu, *Solid State Ionics* 180 (2009) 698–702.
18. Wang Guoping, Zhang Qingtang, Yu Zuolong, Qu MeiZheng, *Solid State Ionics* 179 (2008) 263–268.
19. D. Li, M.B. Müller, S. Gilje, R.B. Kaner, G.G. Wallace, *Nature Nanotechnology* 3 (2008) 101 – 105.
20. Y.R. Jhan, J.G. Duh, *J. Power Sources* 198 (2012) 294–297.
21. Y. Ding, G.R. Li, C.W. Xiao, X.P. Gao, *Electrochim. Acta* 102 (2013) 282–289.
22. N. Zhu, W. Liu, M.Q. Xue, et al, *Electrochim. Acta* 55 (2010) 5813–5818.
23. M. Marinaro, F. Nobili, R. Tossici, R. Marassi, *Electrochim. Acta* 89 (2013) 555–560.
24. A. Varzi, C. Täubert, M. W. Mehrens, *Electrochim. Acta* 78 (2012) 17–26.
25. A.Y. Shenouda, Hua K. Liu, *J. Alloys Compd.* 477 (2009) 498.